

Electronic Supporting Information

Deformation-induced phosphorescence shift in a 2D elastically flexible organic single crystal: Role of chalcogen-centered weak interactions

Subhrajyoti Bhandary,^a Rik Van Deun,^b Anna M. Kaczmarek^c and Kristof Van Hecke^{*a}

^aXStruct, Department of Chemistry, Ghent University, Krijgslaan 281-S3, 9000 Ghent, Belgium

^bL³-Luminescent Lanthanide Lab, Department of Chemistry, Ghent University, Krijgslaan 281-S3, 9000 Ghent, Belgium

^cNanoSensing Group, Department of Chemistry, Ghent University, Krijgslaan 281-S3, 9000 Ghent, Belgium

E-mail: kristof.vanhecke@ugent.be

Table of Contents

Movies S1-S2. Elastic bending of a DBS single crystal on major (101) face

Movies S3-S4. Elastic bending of a DBS single crystal on side (001) face

Movie S5. Elastic bending of a DBS-Br single crystal on major (001) face

Movie S6. Brittle behavior of a DBS-Br single crystal from side (011) face

S1. Materials and crystallization

S2. Single-crystal X-ray diffraction measurements, structure refinement and powder X-ray diffraction

S3. Bending experiments of single crystals under optical microscope

S4. Solid-state photoluminescence of single crystals

S5. Energy framework calculations

S6. References

S1. Materials and crystallization

Dibenzothiophene (DBS) was purchased from Aldrich (D32202-25G) and 2-bromodibenzo[b,d]thiophene (DBS-Br) was purchased from FluoroChem (223072-1G). Both compounds were subsequently recrystallized from a hexane-methanol (3:1) solvent mixture. The recrystallized samples were screened for crystallization in various organic solvents at room temperature (15-18 °C). After crystallization by slow evaporation of benzene as solvent, good quality single crystals of acicular/long plates) for DBS and thin long plates/acicular for DBS-Br were obtained (in both straight and naturally bent morphologies). Such single crystals were used for all further analyses.

S2. Single crystal diffraction measurements, structure refinement, and powder X-ray diffraction

Single crystal X-ray diffraction (SCXRD) data for all single crystals were collected on a Rigaku Oxford Diffraction SuperNova Dual Source (Cu at zero) diffractometer, equipped with an Atlas CCD detector using ω scans and Cu $K\alpha$ radiation ($\lambda = 1.54184 \text{ \AA}$). Data reduction was performed with the Rigaku *CrysAlisPro* Software.^[1] The crystal structures were solved by Intrinsic Phasing using the *ShelXT* program.^[2] All structures were refined by the full-matrix least-squares method using *ShelXL* 2018/3,^[3] via the *Olex2* interface.^[4] All non-hydrogen atoms were refined anisotropically. All hydrogen atoms were positioned geometrically and refined using a riding model.

Powder X-ray diffraction measurements for bulk, recrystallized samples were performed on a Bruker D8 Advance diffractometer using Cu $K\alpha$ radiation ($\lambda = 1.5406 \text{ \AA}$). An excellent agreement of experimental and calculated (from SCXRD) patterns indicated phase purity of their bulk single crystals.

Table S1. Crystal data and structure refinement parameters for DBS and DBS-Br single crystals (straight and naturally bent)

Identification code	DBS	DBS-nat-bent	DBS-Br	DBS-Br-nat-bent
CCDC	2120853	2166318	2120854	2166317
Empirical formula	C ₁₂ H ₈ S	C ₁₂ H ₈ S	C ₁₂ H ₇ BrS	C ₁₂ H ₇ BrS
Formula weight	184.24	184.24	263.15	263.15
Temperature/K	293(2)	290(2)	293(2)	290(2)
Crystal system	<i>monoclinic</i>	<i>monoclinic</i>	<i>orthorhombic</i>	<i>orthorhombic</i>
Space group	<i>P2₁/n</i>	<i>P2₁/n</i>	<i>P2₁2₁2₁</i>	<i>P2₁2₁2₁</i>
a/Å	8.7008(4)	8.7011(5)	3.9779(2)	3.9868(3)
b/Å	6.0100(3)	6.0075(3)	12.1736(4)	12.1976(7)
c/Å	17.1614(9)	17.1510(9)	20.4259(7)	20.4470(11)
α /°	90	90	90	90
β /°	93.687(5)	93.695(5)	90	90
γ /°	90	90	90	90
Volume/Å ³	895.55(8)	894.65(8)	989.13(7)	994.33(10)
Z	4	4	4	4
$\rho_{\text{calc}}/\text{cm}^3$	1.367	1.368	1.767	1.758
μ/mm^{-1}	2.704	2.707	7.220	7.182
F(000)	384.0	384.0	520.0	520.0
Crystal size/mm ³	0.16 × 0.12 × 0.04	0.3 × 0.08 × 0.04	0.18 × 0.12 × 0.03	0.25 × 0.08 × 0.04
Radiation	Cu $K\alpha$ ($\lambda = 1.54184 \text{ \AA}$)	Cu $K\alpha$ ($\lambda = 1.54184 \text{ \AA}$)	Cu $K\alpha$ ($\lambda = 1.54184 \text{ \AA}$)	Cu $K\alpha$ ($\lambda = 1.54184 \text{ \AA}$)
2 θ range for data collection/°	10.33 to 149.226	10.338 to 134.024	8.456 to 147.654	8.44 to 148.108
Index ranges	-10 ≤ h ≤ 10, -7 ≤ k ≤ 7, -20 ≤ l ≤ 21	-10 ≤ h ≤ 10, -7 ≤ k ≤ 7, -20 ≤ l ≤ 19	-4 ≤ h ≤ 4, -14 ≤ k ≤ 14, -25 ≤ l ≤ 24	-4 ≤ h ≤ 4, -14 ≤ k ≤ 12, -24 ≤ l ≤ 25

Reflections collected	8216	8404	8723	4820
Independent reflections	1802 [$R_{\text{int}} = 0.0389$, $R_{\text{sigma}} = 0.0308$]	1591 [$R_{\text{int}} = 0.1776$, $R_{\text{sigma}} = 0.0565$]	1953 [$R_{\text{int}} = 0.0516$, $R_{\text{sigma}} = 0.0360$]	1831 [$R_{\text{int}} = 0.0731$, $R_{\text{sigma}} = 0.0553$]
Data/restraints/parameters	1802/0/119	1591/0/118	1953/0/127	1831/0/127
Goodness-of-fit on F^2	1.087	1.541	1.042	1.204
Final R indexes [$I \geq 2\sigma(I)$]	$R_1 = 0.0362$, $wR_2 = 0.0895$	$R_1 = 0.1433$, $wR_2 = 0.4136$	$R_1 = 0.0315$, $wR_2 = 0.0728$	$R_1 = 0.1028$, $wR_2 = 0.2940$
Final R indexes [all data]	$R_1 = 0.0494$, $wR_2 = 0.1034$	$R_1 = 0.1666$, $wR_2 = 0.4727$	$R_1 = 0.0418$, $wR_2 = 0.0802$	$R_1 = 0.1245$, $wR_2 = 0.3580$
Largest diff. peak/hole / $e \text{ \AA}^{-3}$	0.22/-0.24	0.88/-1.37	0.29/-0.33	1.59/-0.41
Flack parameter	NA	NA	0.01(2)	-0.04(8)

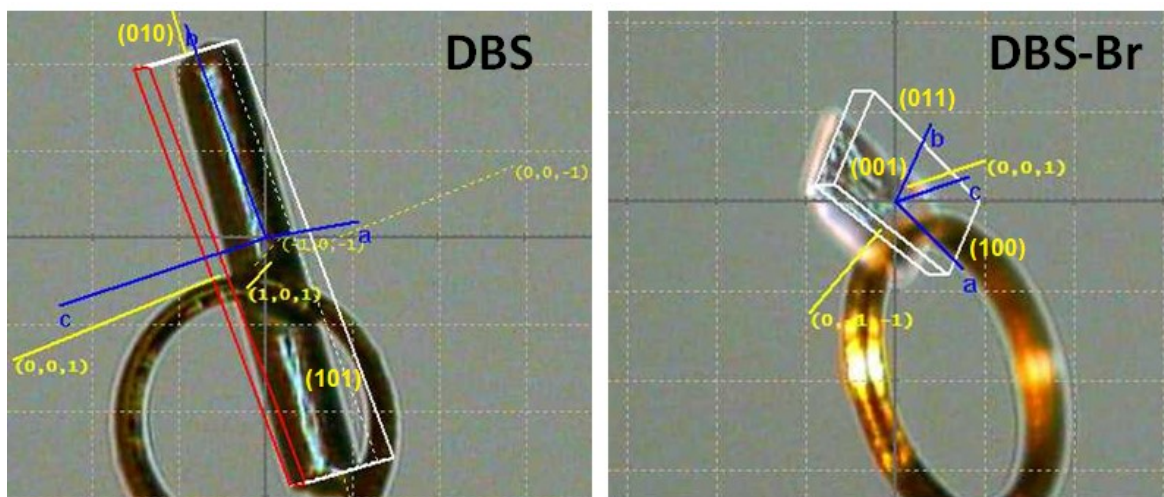


Figure S1. Experimental face indexing of DBS and DBS-Br single crystals. Bendable faces are (101)/(001) and (001), for DBS and DBS-Br, respectively.

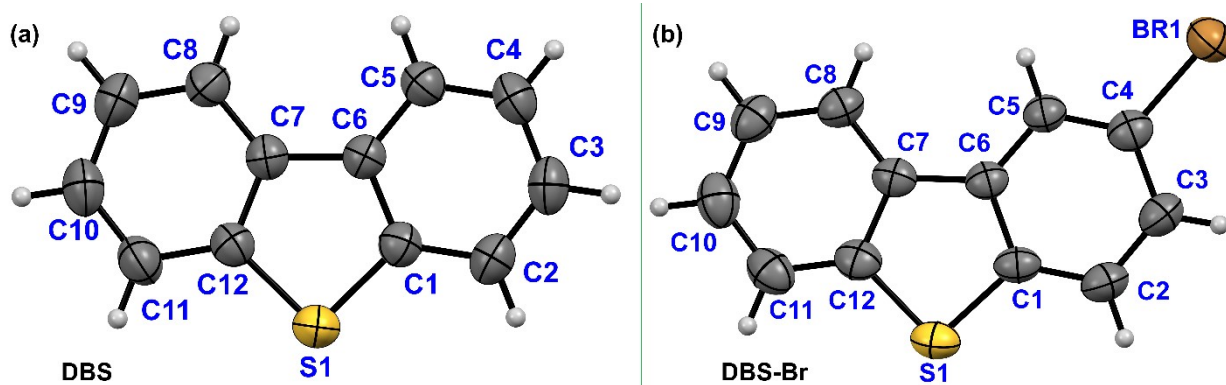


Figure S2. Molecular structures of DBS (a) and DBS-Br (b) single crystals, showing thermal displacement ellipsoids (drawn at the 50% probability level) and atom numbering scheme.

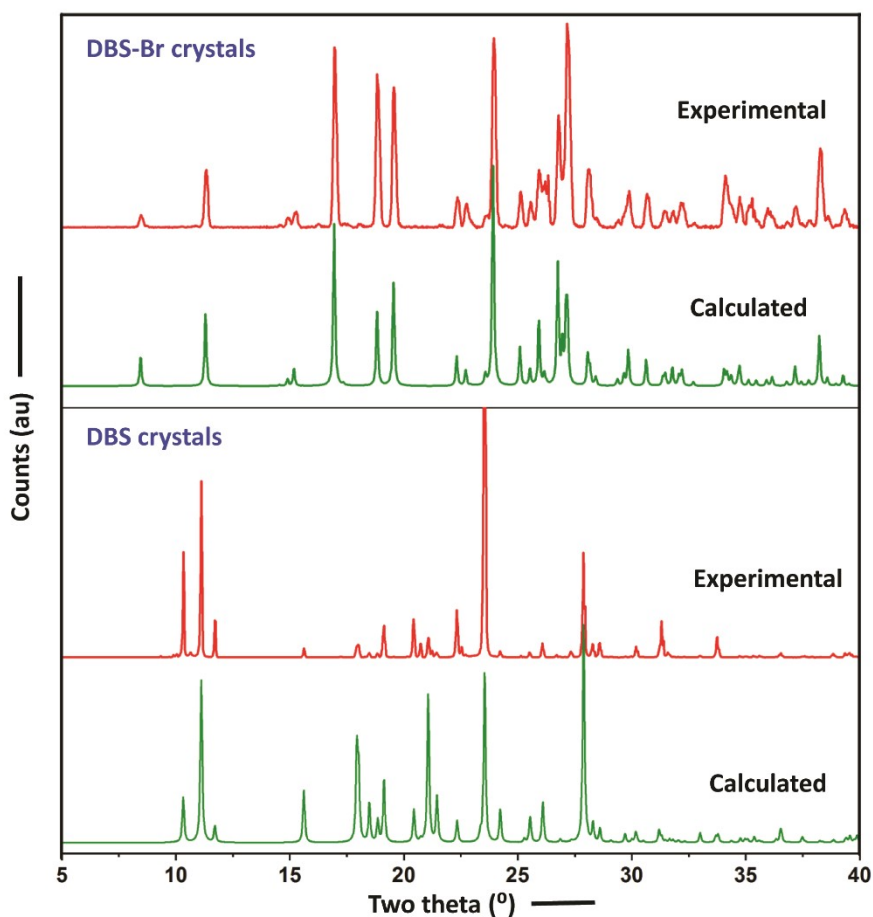


Figure S3. Overlay of experimental (red) and calculated (green) PXRD patterns of recrystallized DBS and DBS-Br compounds showing their phase purity.

Table S2. List of important intermolecular interactions (with geometrical parameters: distance and angle) present in crystals of DBS and DBS-Br and their interaction energies (IE) [Cg1- C1 > C6, Cg2- C7 > C12, Cg3- C1_C6_C7_C12_S1]. C-H distances are *neutron normalized*.

Motif	Symmetry	D...A (Å)	H...A (Å)	D-H...A (°)	IE (kJ/mol)
DBS					
C8-H8... π (C5) C5-H5... π (C6)	$-x+1/2, y+1/2, -z+1/2$	4.056(3) 3.768(2)	2.99 2.82	166 145	-26.0
S1... π (C5) S1... π (C8) Displaced stacking	$x, y+1, z$	3.632(2) 3.706(2)	- -	- -	-16.1
S1... π (C3) C2-H2... π (C2)	$-x+1/2, y+1/2, -z+1/2$	3.576(3) 3.977(3)	- 2.99	149 (C12-S1-C3) 151	-13.4
C11-H11...S1 (dimer)	$-x, -y, -z$	4.047(1)	2.99	165	-5.0
Cg2...Cg2 stacking	$-x, -y, -z$	4.028(3)	-	-	-20.6
H3...H11 H3...H10	$x+1/2, -y+1/2, z+1/2$	2.537(2) 2.507(2)	- -	- -	-4.2
H3...H9 H4...H10	$x+1/2, -y+1/2, z+1/2$	2.618(2) 2.518(2)	- -	- -	-4.3

$\pi(\text{C9})\cdots\pi(\text{C10})$ displaced stacking	$-x, -y, -z$	3.857(3)	-	-	-7.4
DBS-Br					
S $\cdots\pi(\text{Cg2})$ Cg1 $\cdots\text{Cg1}$ Cg2 $\cdots\text{Cg2}$	$x+1, y, z$	3.574(4) 3.978(8) 3.978(8)	-	-	-36.7
C8-H8 $\cdots\text{S1}$ C5-H5 $\cdots\text{S1}$ C8-H8 $\cdots\pi(\text{C1})$ C11-H11 $\cdots\text{Br1}$	$-x, y+1/2, -z+1/2$	4.133(5) 3.976(4) 4.131(5) 3.844(5)	3.08 2.92 3.10 3.22	163 165 159 118	-14.7
C2-H2 $\cdots\pi(\text{C9})$ C8-H8 $\cdots\text{S1}$ C5-H5 $\cdots\text{S1}$	$-x, y+1/2, -z+3/2$	3.948(5) 3.714(5) 3.675(5)	2.88 3.16 3.12	168 112 112	-15.4
C3-H3 $\cdots\text{Br1}$ C3-H3 $\cdots\pi(\text{C3})$	$x+1/2, -y+1/2, -z$	3.921(4) 4.182(4)	3.05 3.27	137 141	-9.0
C9-H9 $\cdots\text{Br1}$ C10-H10 $\cdots\text{Br1}$	$-x+1/2, -y, z+1/2$	4.140(5) 3.772(5)	3.21 3.17	143 115	-6.0
C10-H10 $\cdots\pi(\text{C11})$ C10-H10 $\cdots\pi(\text{C10})$	$x+1/2, -y+1/2, -z$	4.071 3.93	3.17 3.12	140 132	-4.7

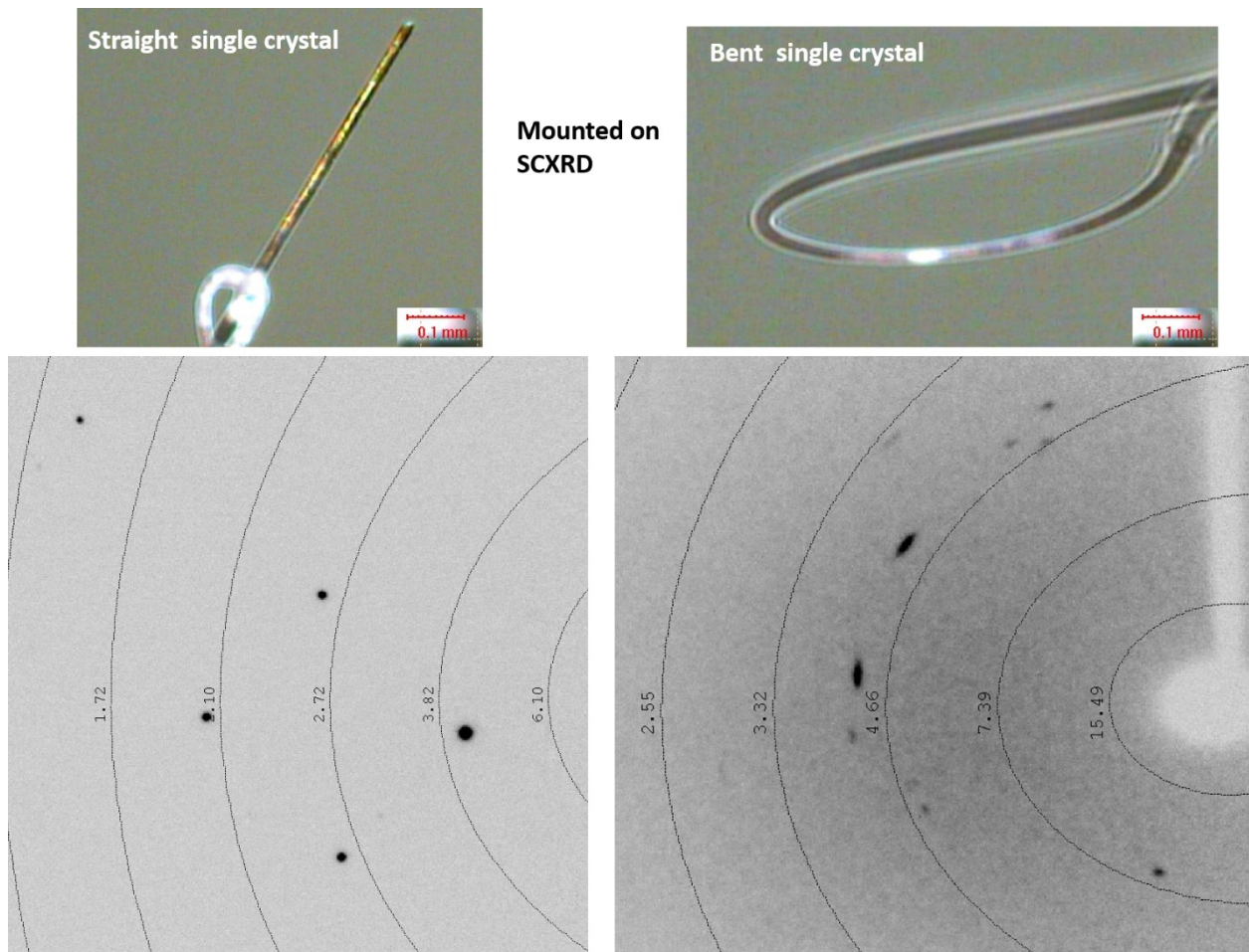


Figure S4. Comparison of diffraction patterns in SCXRD for a straight and an elastically bent [on major (101) face] DBS single crystal loop, mounted on a diffractometer. Note the broad/mosaic diffraction spots in case of the bent crystal at low angles.

S3. Bending experiments of single crystals under optical microscope

Crystal bending experiments were performed using a three-point bending method. Good (macroscopic) quality single crystals were placed on a glass microscope slide, immersed in a little amount of Paratone oil (Hampton Research) to prevent crystal damage due to friction. The above mentioned set up was viewed with an Olympus SZ61-TR optical stereomicroscope, equipped with a Dino-Eye Edge eyepiece USB camera and Dino Capture (2.0) software. A single crystal was stabilized from one side with a pair of metal tweezers, while mechanical force was gradually applied from the opposite face by a metal needle. The elastic strain was quantified at the point of maximal curvature using the *Euler-Bernoulli* equation [see equation 1]. The thickness (d) and radius (R) of curvature of the bent crystals prior to breakage were measured using the Dino Capture (2.0) software.

$$\text{Elastic strain, } E (\%) = \frac{d}{2R} \times 100 \quad [1]$$

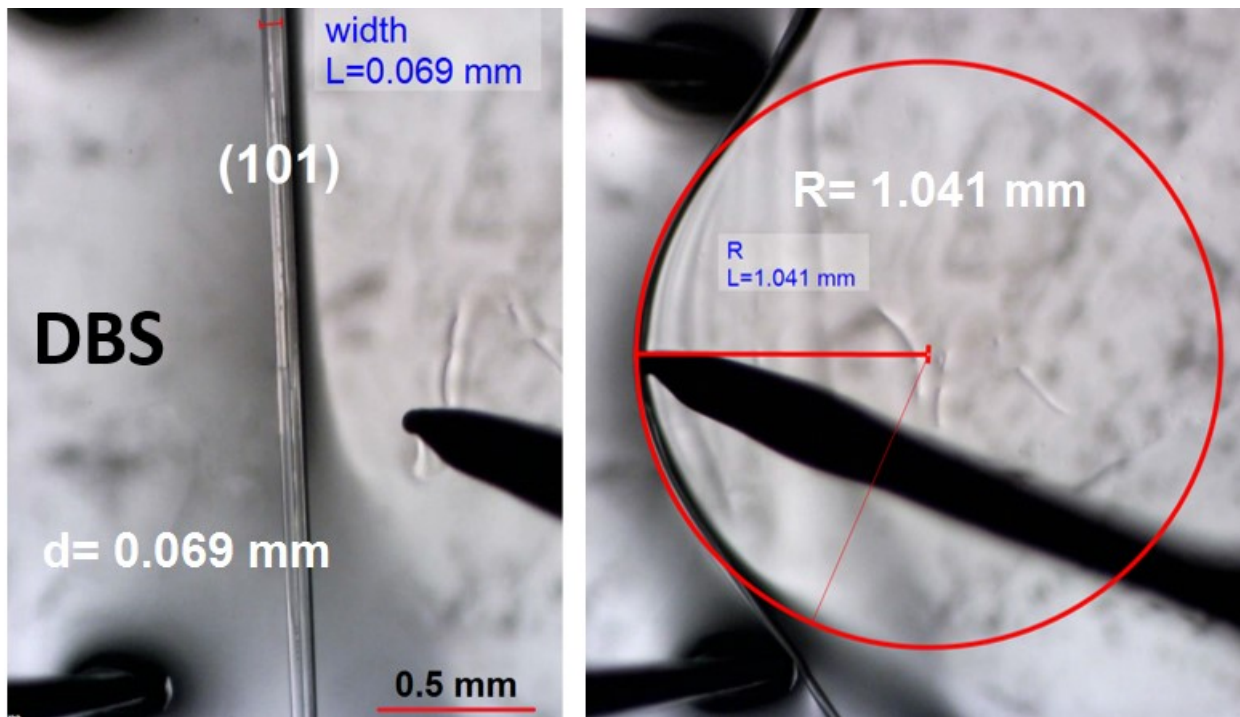


Figure S5. Elastic strain (E) calculation on major (101) face of a DBS single crystal; $E = 3.3\%$.

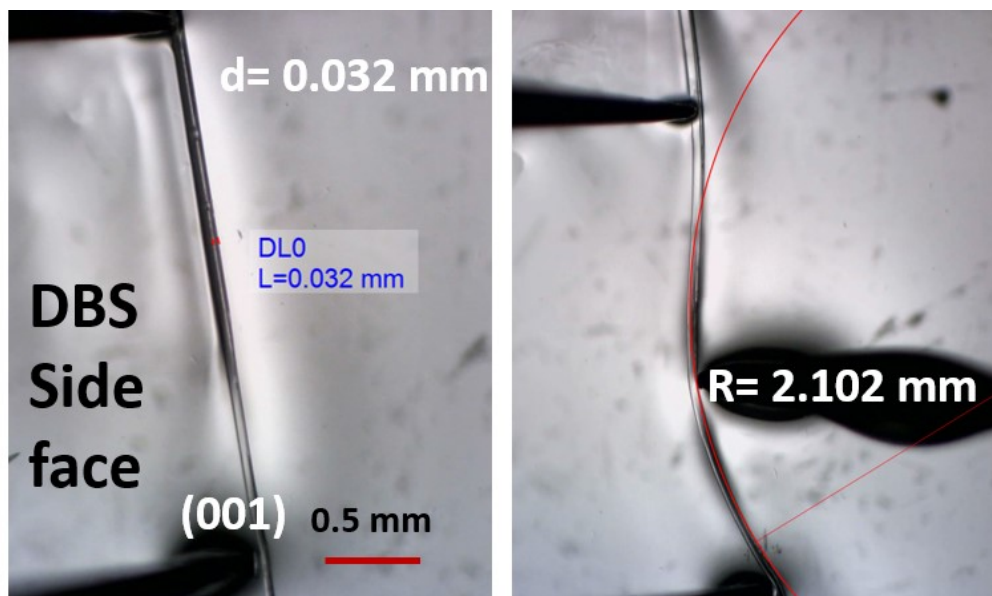


Figure S6. Elastic strain (E) calculation on side (001) face of a DBS single crystal; $E = 0.8\%$.

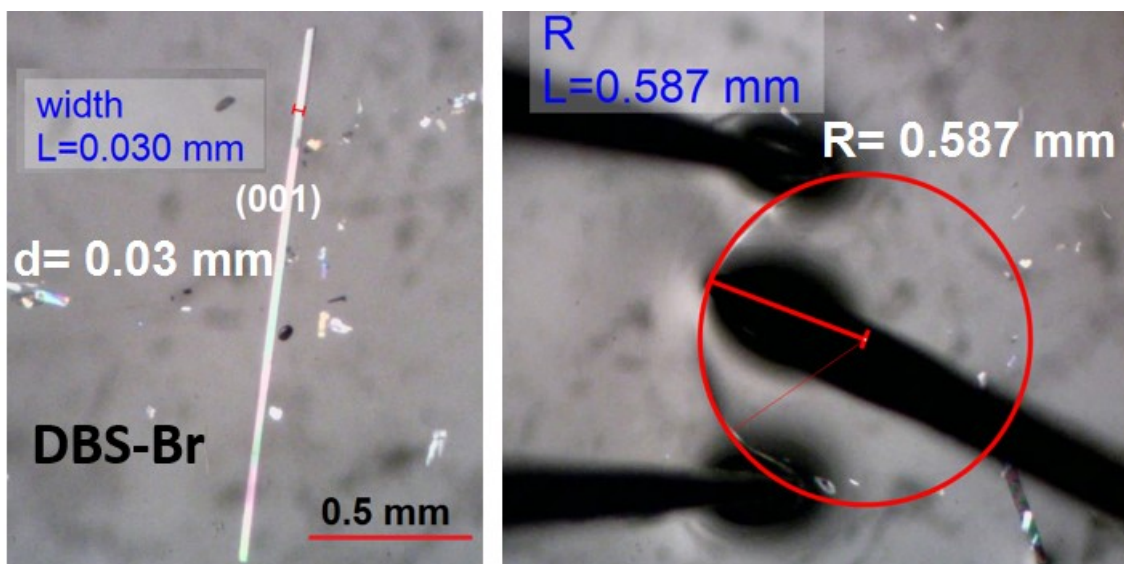


Figure S7. Elastic strain (E) calculation on major (001) face of a DBS-Br single crystal; $E = 2.5\%$.

S4. Solid-state photoluminescence of single crystals

Steady-state photoluminescence (PL) measurements on *one single crystal* of each compound were performed at room temperature using an Edinburgh FLSP920 spectrophotometer equipped with a Hamamatsu R928P PMT detector. The single crystals were mounted between quartz plates for all PL measurements. The PL spectra were acquired with a 450 W continuous-wave Xenon lamp as an excitation source. In order to map the effect of bending, an elongated straight (~ 4 mm), their elastically bent and a naturally bent (~ 3 mm) single crystals of DBS were taken for PL measurements (Figure S11). Luminescence decay times were measured using a pulsed 60 W microsecond flashlamp (repetition rate 0.1-100 Hz, pulse width 1.5-2.5 μ s).

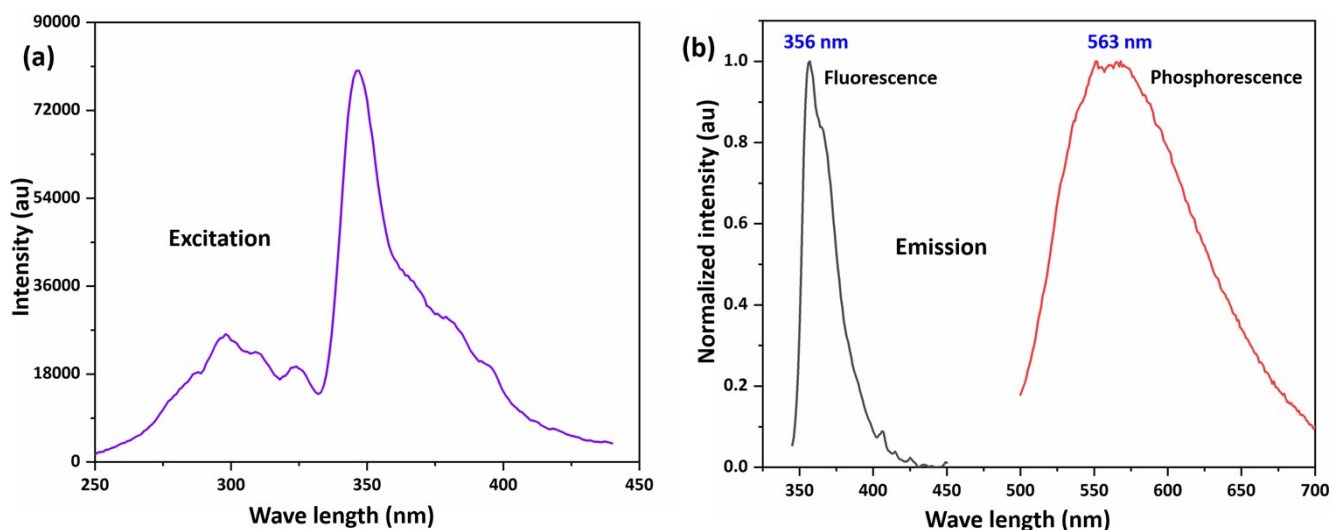


Figure S8. Excitation (a) and emission (b) spectra of one pristine (straight) single crystal of DBS. Black and red curves indicate fluorescence (peak at 356 nm) and phosphorescence (peak at 563 nm) spectra, respectively. The single crystal was excited (λ_{exc}) at 300 nm.

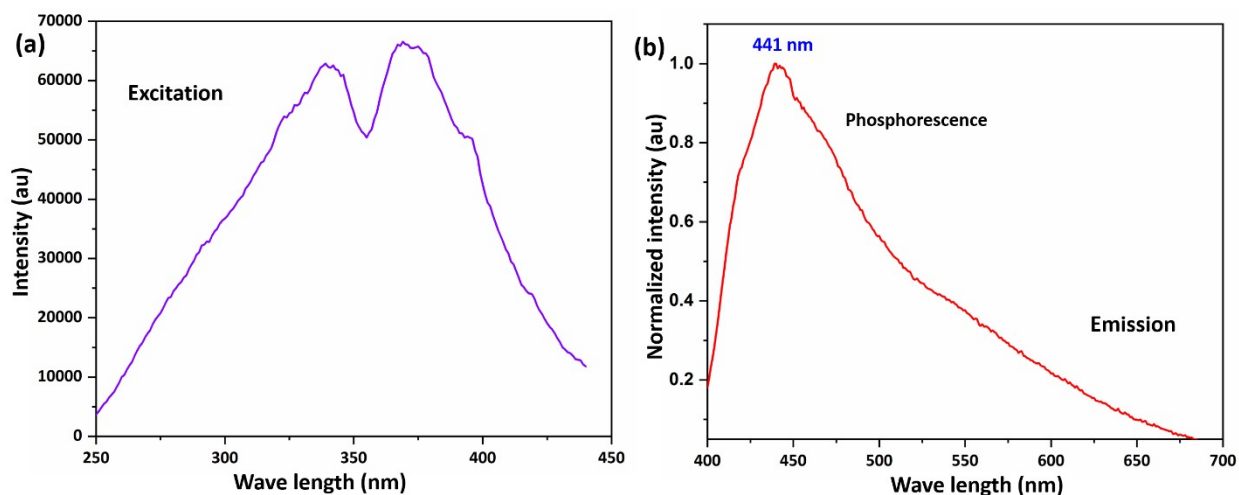


Figure S9. Excitation (a) and emission (b) spectra of one pristine single crystal of DBS-Br. The red curve indicates the phosphorescence (peak at 441 nm) spectrum. The single crystal was excited (λ_{ex}) at 371 nm.

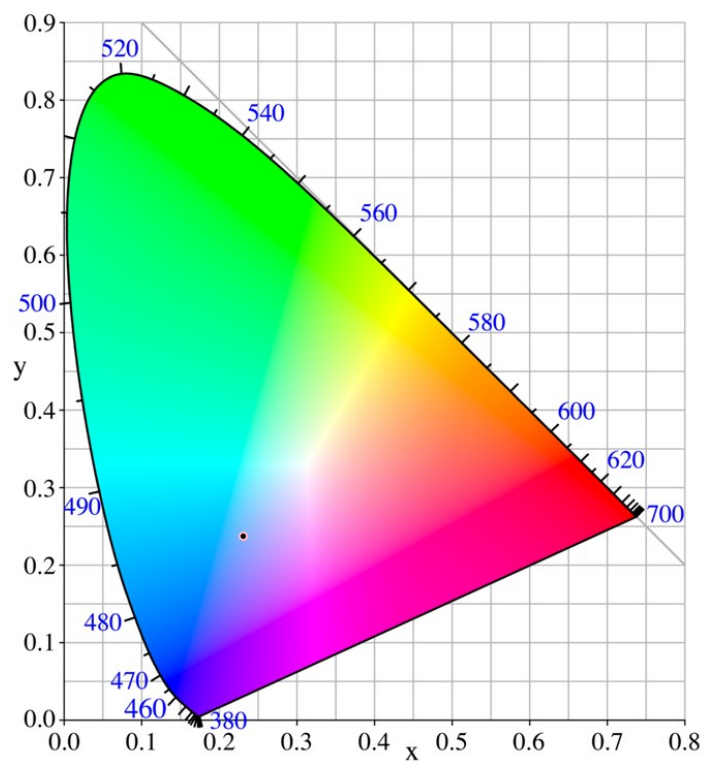


Figure S10. Plot of CIE coordinates (0.23, 0.23) for DBS-Br, showing blue emission from single crystals.

Table S3. Photoluminescence lifetimes for DBS and DBS-Br single crystals at room temperature.

Single crystal	Peak	Average lifetime, $\langle\tau\rangle^*$
DBS	563 nm	11.6 μs
DBS-Br	441 nm	8.7 μs

* Such microsecond decay lifetimes suggest both DBS and DBS-Br single crystals are short-lived phosphorescent. $\langle\tau\rangle$ was obtained from the double-exponential fit of their decay curves, $\langle\tau\rangle = (\tau_1^2 A_1 + \tau_2^2 \cdot A_2) / (\tau_1 \cdot A_1 + \tau_2 \cdot A_2)$

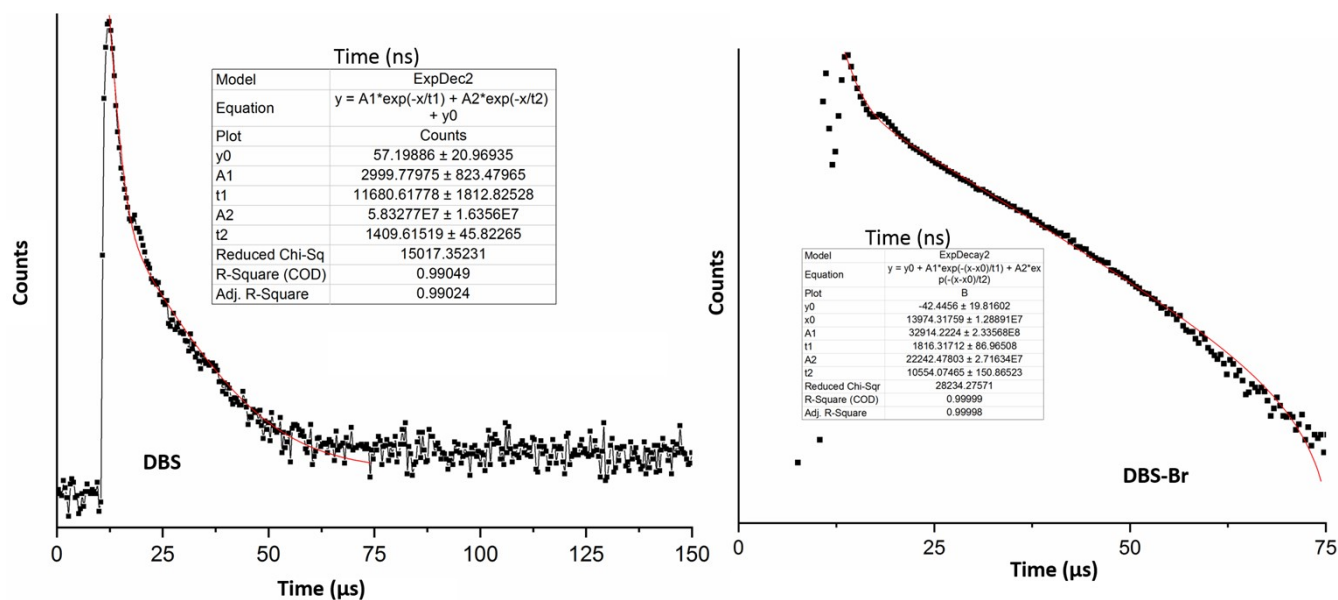


Figure S11. Fitting of time-resolved phosphorescence decay profiles for each DBS (peak at 563 nm) and DBS-Br (peak at 441 nm) single crystal.

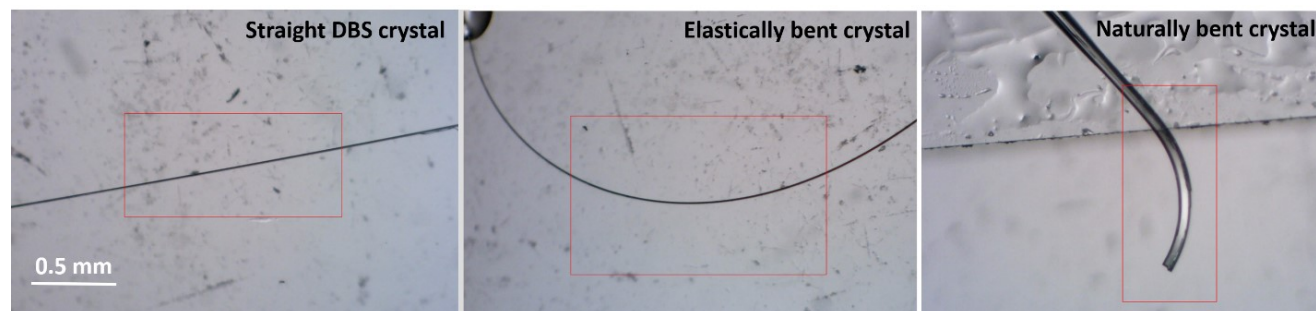


Figure S12. Different shapes of (elongated straight, elastically and naturally bent) DBS single crystals used for PL measurements. One single crystal was used per measurement at ambient temperature. Red rectangles indicate probe region of crystal in PL measurements. Elastic deformation was made on major (101/-10-1) face. DBS crystal (used in PL measurement) was mechanically deformed up to calculated elastic strain (E) of around 2%.

S5. Energy framework calculations

Energy frameworks, for both DBS and DBS-Br crystals, were constructed from pairwise intermolecular interaction energy calculations (at the crystal geometry) using the CE-B3LYP/ DGDZVP molecular wave functions in *CrystalExplorer21.5*.^[5] Frameworks are shown at an energy cut-off of -8 kJ/mol and tube size of 100.

Output of interaction energy calculations in *CrystalExplorer 21.5*:

DBS

	N	Symop	R	Electron Density	E_ele	E_pol	E_dis	E_rep	E_tot
	2	-x+1/2, y+1/2, -z+1/2	5.12	B3LYP/DGDZVP	-12.2	-1.7	-34.9	30.0	-26.0
	1	-x, -y, -z	9.56	B3LYP/DGDZVP	-3.4	-0.3	-7.8	5.2	-7.4
	0	-x, -y, -z	11.61	B3LYP/DGDZVP	0.7	-0.0	-1.0	0.0	-0.2
	0	-x, -y, -z	7.79	B3LYP/DGDZVP	-2.6	-0.4	-8.5	8.7	-5.0
	0	-x+1/2, y+1/2, -z+1/2	7.23	B3LYP/DGDZVP	-8.5	-0.9	-16.1	16.6	-13.4
	1	x, y, z	6.01	B3LYP/DGDZVP	-9.9	-1.0	-19.4	19.3	-16.1
	1	x+1/2, -y+1/2, z+1/2	10.15	B3LYP/DGDZVP	-0.2	-0.4	-7.5	4.7	-4.2
	1	x+1/2, -y+1/2, z+1/2	10.51	B3LYP/DGDZVP	-0.1	-0.3	-7.2	3.8	-4.3
	0	-x, -y, -z	5.67	B3LYP/DGDZVP	-10.7	-1.6	-30.9	30.4	-20.6

DBS-Br

	N	Symop	R	Electron Density	E_ele	E_pol	E_dis	E_rep	E_tot
	0	x, y, z	3.98	B3LYP/DGDZVP	-19.2	-1.6	-57.3	56.1	-36.7
	0	-x, y+1/2, -z+1/2	6.97	B3LYP/DGDZVP	-9.0	-1.0	-19.3	18.9	-15.4
	0	x+1/2, -y+1/2, -z	8.47	B3LYP/DGDZVP	-4.8	-0.6	-10.5	9.1	-9.0
	0	-x+1/2, -y, z+1/2	11.02	B3LYP/DGDZVP	-4.5	-0.3	-7.7	9.1	-6.0
	0	x+1/2, -y+1/2, -z	12.75	B3LYP/DGDZVP	-0.9	-0.4	-6.9	4.2	-4.7
	0	-x, y+1/2, -z+1/2	6.63	B3LYP/DGDZVP	-8.5	-1.2	-20.8	21.5	-14.7
	0	-x+1/2, -y, z+1/2	11.52	B3LYP/DGDZVP	-1.2	-0.1	-4.0	2.2	-3.4

An elastically bent single crystal of DBS/DBS-Br

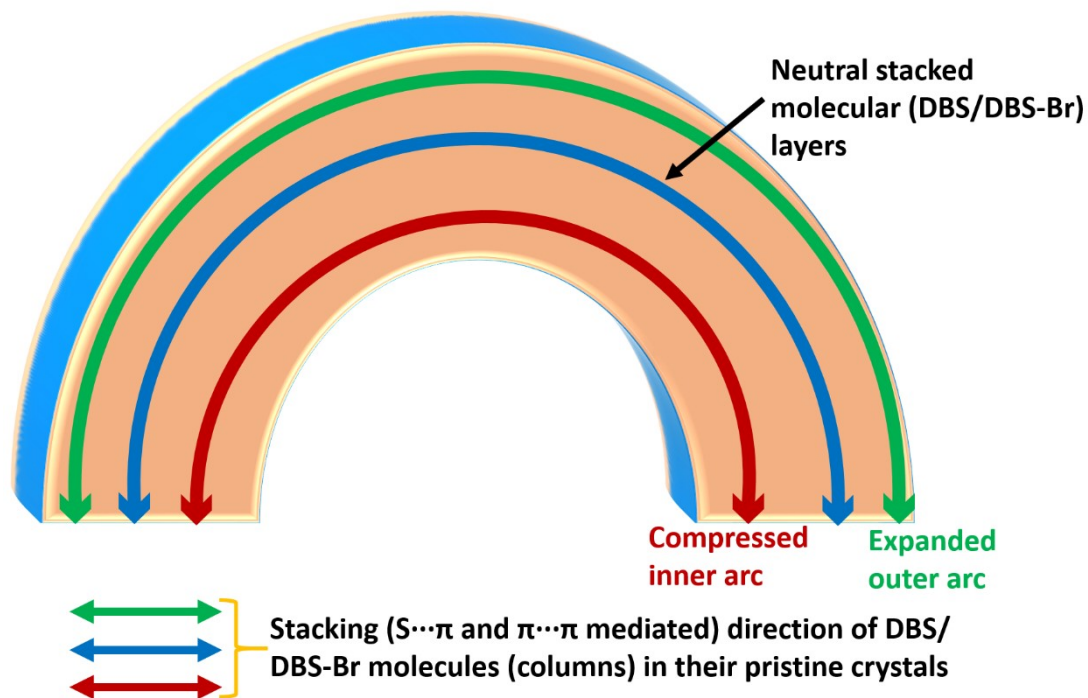
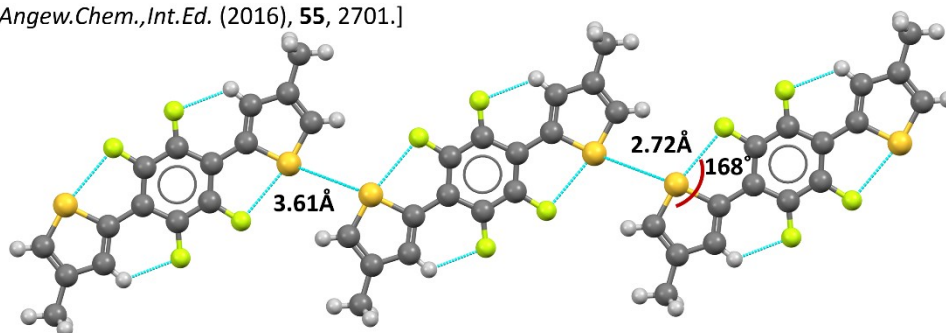


Figure S13. Schematic molecular level situation for elastic bending of a DBS/DBS-Br single crystal. Blue and pink shades indicate major and lateral faces of the single crystal, respectively. DBS/DBS-Br molecules are stacked in columnar fashion (double-headed blue arrows) via chalcogen involved interactions along the long axis of their single crystals.

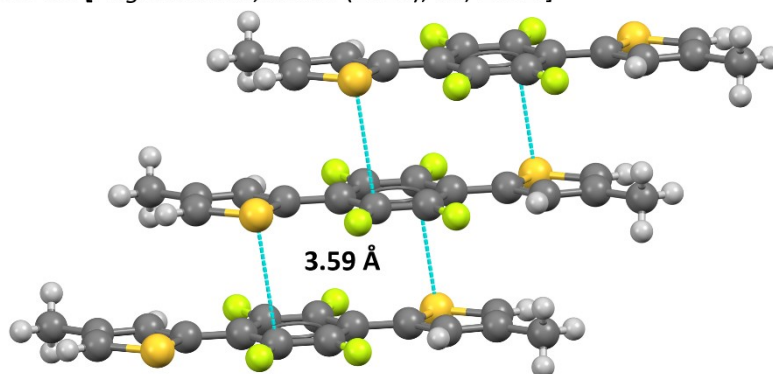
VEXPOG

[*Angew.Chem.,Int.Ed.* (2016), 55, 2701.]



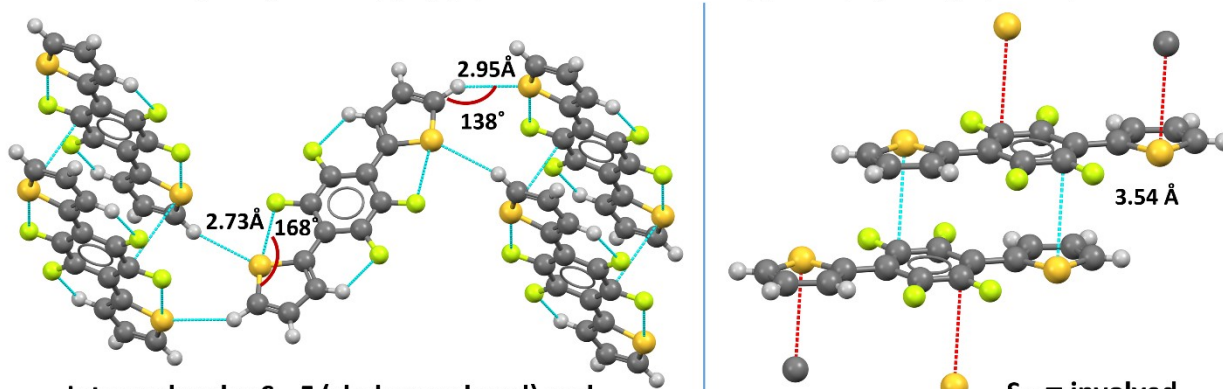
$S\cdots S$ (type I) chain and intramolecular $S\cdots F$ interactions (chalcogen bond)

VEXPOG [*Angew.Chem.,Int.Ed.* (2016), 55, 2701.]



S... π mediated stacking

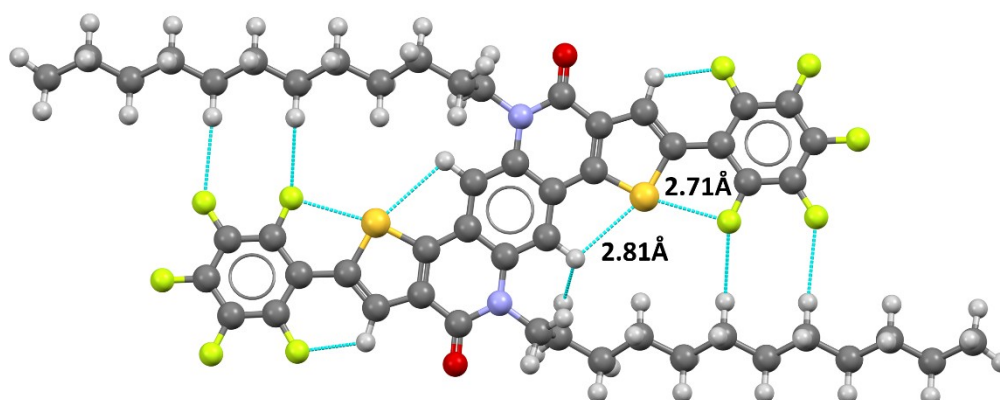
1,4-bis(thien-2-yl)-2,3,5,6-tetrafluorobenzene; [*Sci Rep.* (2017), 7, 9453.]



Intramolecular S...F (chalcogen bond) and intermolecular C-H...S interactions

S... π involved stacking

QIJROT01 [*Angew.Chem.,Int.Ed.* (2018), 57, 17002.]



Intramolecular C-H...S interaction and S...F chalcogen bond

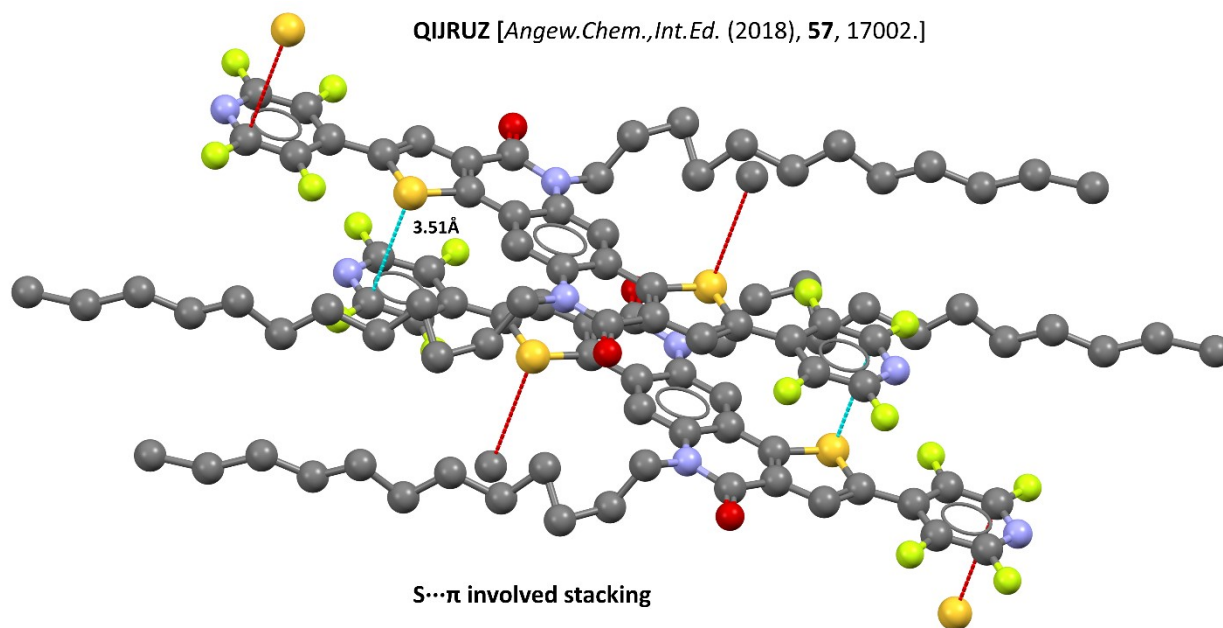


Figure S14. Previously reported elastically flexible different π -conjugated fluorescent crystals, having thiophene moieties and showing formation of chalcogen-centered S...F (intra), S... π stacking, S...S, and C-H...S interactions.

S6. References

- [1] Agilent, **2014**, *CrysAlis PRO*. Agilent Technologies Ltd, Yarnton, Oxfordshire, England.
- [2] G. M. Sheldrick, *Acta Crystallogr A Found Adv.* **2015**, *71*, 3-8.
- [3] G. M. Sheldrick, *Acta Crystallogr C Struct Chem.* **2015**, *71*, 3-8.
- [4] O. V. Dolomanov, L. J. Bourhis, R. J. Gildea, J. A. K. Howard and H. Puschmann, *J. Appl. Crystallogr.* **2009**, *42*, 339-341.
- [5] C. F. Mackenzie, P. R. Spackman, D. Jayatilaka, M. A. Spackman, *IUCrJ*, **2017**, *4*, 575-587.